2021 18th International Conference on Electrical Engineering, Computing Science and Automatic Control (CCE)
Mexico City, Mexico. November 10-12, 2021

Optoelectronic properties of Sb_2S_3 thin films grown by Physical Vapor Deposition

J. Cruz-Gómez
Facultad de Química
UAQ
Santiago de Querétaro, Qro. México
jorge_jcg@icloud.com

E. Hernández-Cantero
Facultad de Química
UAQ
Santiago de Querétaro, Qro. México
ehernandez136@alumnos.uaq.mx

D. Santos-Cruz
Dep. de Ingeniería Eléctrica
CINVESTAV-IPN, SEES
Mexico City, Mexico
dsantos@cinvestav.mx

S.A. Mayén-Hernández
Facultad de Química
UAQ
Santiago de Querétaro, Qro. México
sandra.mayen@uaq.edu.mx

F. DeMoure-Flores
Facultad de Química
UAQ
Santiago de Querétaro. Qro. México
francisco.javier.demoure@uaq.mx

J. Santos-Cruz
Facultad de Química
UAQ
Santiago de Querétaro. Qro. México
jsantos@uaq.edu.mx

Abstract*— Antimony (III) sulfide thin films are prepared on glass substrates by physical vapor deposition technique. Then, the films are annealed at different temperatures from 250 to 400°C with N_2 and N_2-S atmosphere. The effect of annealing temperature on the optoelectronic properties is investigated. The films are characterized by ultraviolet-visible spectroscopy, Raman spectroscopy, XRD, EDS analysis and Hall effect. The film annealed at 300°C in an N_2 atmosphere exhibited the best condition with an initial thickness of 400 nm and band gap of 1.76 eV. Also, stibnite phase, the charge carrier concentration of $1.25x10^{12}$ cm^{-3} with a p-type conductivity, the resistivity of $3.9x10^5$ Ω-cm, and mobility of 18.11 $cm^2V^{-1}s^{-1}$ are obtained.

Keywords—Sb_3S_2, Stibnite, chalcogenide, semiconductor material

I. INTRODUCTION

Antimony III sulfide (Sb_2S_3) is a chalcogenide that gains intense interest among the scientific community due to its abundant in the earth crust (Sb and S, 0.2 and 260 ppm respectively [1,2]) including an environmentally friendly constituent, simple and stable phase with a low melting point (550 °C [1]), and its excellent optics and electronic properties which make it a suitable candidate for solar cell applications. Besides, Sb_2S_3 is a semiconductor composed of an orthorhombic crystal structure that belongs to the V-VI group. It occurs naturally in the earth's crust as a mineral called Stibnite, which indicates thermodynamic stability [3]. In the thin film, a Stibnite or Antimony sulfide (Sb_2S_3) is generally used as a sensitizing and absorbent layer in solar cells, resulting in energy conversion efficiency of up to 7.5% [4]. Antimony sulfide exhibits distinctive properties, including a direct optical bandgap (1.5 to 1.8 eV), high optical absorption coefficient a>10^5 cm^{-1}, with a work function of 5.26 eV, the electronic affinity of 4.87 eV and simple processing with stability and abundant constituents [1-4]. Furthermore, antimony sulfide-based solar cells have shown excellent performance to date, making them a promising solar cell material for further development. Antimony sulfide thin films have been prepared by several methodologies and techniques such as Sputtering [3], Chemical Bath deposition [4], Spin Coating [5], Spray Pyrolysis [6], Pulsed Laser Ablation [7] and Thermal evaporation [1] and most importantly post treatment process (> 250°C) were done to crystallize the Sb_2S_3 [2].

II. METHODOLOGY

A. Preparation of thin films

Antimony chalcogenide films were obtained by a procedure similar described in [7]. The procedure consisted of two main stages, deposition of antimony sulfide films and thermal treatment of the films in N_2 and N_2-S atmospheres.

In the first stage, glass substrates were cleaned with soap, treated with chromic acid for 24 hours and subsequently attacked with a nitric acid solution (3:1) close to the boiling point for 3 hours. The films were deposited on the corning-glass substrates by physical vapor deposition technique using antimony (III) sulfide (Sb_2S_3) powder purchased from Sigma-Aldrich. For the deposition, initial pressure of 5 x 10^{-5} mbar and the current of 120 A were employed. The distance between the source to the substrate was 16 cm. The Sb_2S_3 film thickness was adjusted to 400 nm.

In the second stage, thermal annealing was carried out at different temperatures from 250 to400°C for 2 hours in a quartz tubular furnace (Lindberg Blue M.) with N_2 and N_2-S atmospheres.

Characterization techniques

The thicknesses of the samples were measured using D-100 KLA Tencor profiler. Raman spectroscopy measurements were acquired with a Thermo Scientific DXR2 system equipped with a 633 nm laser as an excitation source. The transmittance of films was obtained using Genesys 10S UV-VIS, Thermo Scientific. The electrical properties were measured using a Hall Effect Measurement System (ECOPIA HMS-300). The elemental composition of the samples was determined by energy dispersive spectroscopy, EDS analysis in a Hitachi SU1510.

III. RESULTS AND DISCUSSION

A. X-Ray Diffraction characterization

978-1-6654-0029-9/21/$31.00 ©2021 IEEE

Figure 1 shows the XRD patterns of the samples annealed at 300 and 350°C in a) Nitrogen (N) and b) Nitrogen-Sulfur (NS) atmospheres, respectively. In both atmospheres, well-defined diffraction planes of (020), (120), (220), (230), (211), (221), (240), (520), (511) and (611) were obtained, which matches with orthorhombic phase and spacial group Pbnm(62) known as Stibnite (Card PDF#42-1393) Antimony II sulfide. For NS atmosphere, improvement in the crystallinity was observed, the intensity of (020) plane (Fig. 1 b) was increased 3 times for 350°C. The preferential orientation was attained for (020) plane in all cases, this behavior is observed in thermal evaporations thin films among others [1,4].

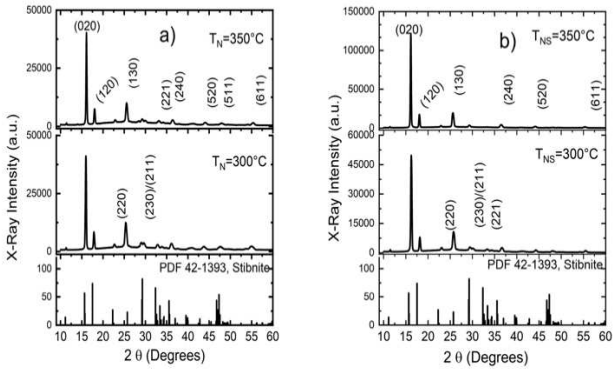

Fig. 1. XRD patterns annealed at 300 and 350°C in a) nitrogen and b) nitrogen-sulfur atmospheres.

The crystallite size (D), strain (ε) and dislocation lines (Δ) were computed for the Debye-Scherrer D= Kλ/βcosθ where D crystallite size, K=0.9, λ, wavelength of the copper 0.154 nm, β full height at a half maximum and θ the Bragg angle, ε= β cosθ/4 and $\Delta=D^{-2}$ [11] formulas respectively. Table I shows the results for the samples annealed in nitrogen and nitrogen-sulfur atmospheres. The crystallite size increases as a function of temperature in both atmospheres. The film annealed at 350°C under nitrogen-sulfur atmosphere (NS) exhibited the highest crystallite size of 37 nm, minimum strain and minimum dislocation lines of 0.933 and $7.3x10^{14}$ lines/m^2, respectively. The results indicate that film annealed at 350°C with NS atmosphere showed better structural properties.

Table I. Crystallite size, strain, a dislocation lines results for the samples annealed at 300 and 350°C in nitrogen and nitrogen-sulfur atmospheres.

Sample	D (nm)	ε $x10^{-3}$	Δ $x10^{15}$ (lines/m^2)
300 N	30.53	1.14	1.07
350 N	33.85	1.02	0.87
300 NS	29.40	1.18	1.16
350 NS	37.14	0.933	0.73

B. Raman characterization

Fig. 2 shows the Raman spectra of the samples obtained with a 632 nm laser: all the samples showed the characteristics of the vibrational mode of the Stibnite. By first-principles studies, the stibnite phase found 30 actives Raman modes Γ_{Raman} = 10Ag + 5B1g + 10B2g + 5B3g) [9, 10], in the present work, only five modes are visible, such as A_g/B_{2g} at 155.56 cm^{-1} assigned to lattice mode, B_{1g} at 192 cm^{-1} corresponds to antisymmetric S-Sb-S bending, B_{1g}/B_{3g} at 238 cm^{-1} related to symmetric S-Sb-S bending, A_g/B_{2g} at 281 cm^{-1} as antisymmetric S-Sb-S stretching mode, and A_g/B_{2g} at 309 cm^{-1} ascribed to symmetric S-Sb-S stretching mode which matches well with the existing report[8,10]. Figure 2 a) displays the samples annealed at different temperatures in a) nitrogen and b) nitrogen-sulfur atmosphere, respectively. The samples annealed in a nitrogen-sulfur atmosphere shows a better Raman intensity, and the FWHM of the vibrational modes at 238 cm^{-1} are 20 - 22 cm^{-1} which confirms the better polycrystallinity of the samples.

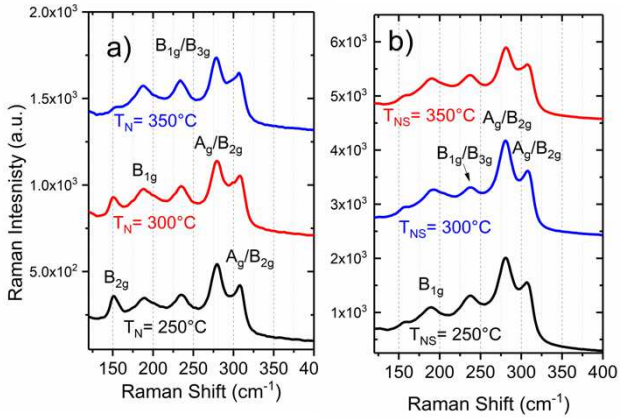

Fig. 2. Raman spectra of a) nitrogen and b) nitrogen-sulfur samples as a function of temperature.

C. Optical characterization

Figure 3 shows the transmittance spectra of the samples annealed in (a) nitrogen and (b) nitrogen-sulfur atmospheres respectively and (c) band gap by Tauc theory of parabolic bands as a direct band gap semiconductor. The samples annealed in nitrogen atmosphere demonstrated the maximum transmittance in the order of 35 %, the absorption edge did not show significant difference as a function of annealed temperature (654 nm). The samples annealed in a nitrogen-sulfur atmosphere revealed the increment in the transmittance up to 55 %, and the absorption edge at 664 nm approximately. This behavior is similar to film annealed at nitrogen atmosphere. From Figure 3 c), it is observed that the band gap changed from 1.74 to 1.76 eV for the film annealed under a nitrogen (N) atmosphere and the band gap varied between 1.78 and 1.81 eV for film annealed with nitrogen-sulfur (NS) atmosphere. The obtained band gap results were similar for both annealing temperature of 350 and 300 °C. These results are consistent with samples grown by thermal evaporation [1-3] technique.

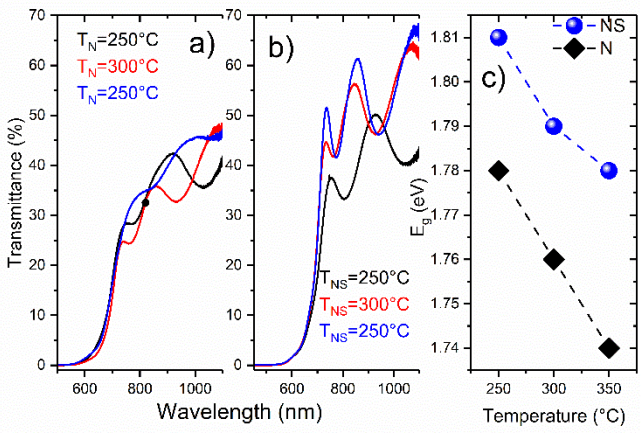

Fig. 3. Transmittance spectra of the samples annealed in a) nitrogen b) nitrogen-sulfur atmospheres, and c) bandgap of the thin films as a function of the annealing temperature.

D. Electrical characterization

Figure 4 shows the electrical measurements carried out using the Hall effect. Samples of 1 x1 cm were employed in the van de Pauw configuration. The obtained charge carrier concentration was varied from $1.18x10^{12}$ to $4.8x10^{12}$ cm^{-3} for the films annealed under nitrogen and nitrogen-sulfur atmospheres. The obtained results are matched with the literature [4, 8-11]. All the samples depicted p-type conductivity due to sulfur deficiency, where the majority charge carries holes provided by sulfur. Therefore, it agrees with the existing report [10], where they explained theoretically that sulfur deficiency decreases the concentration of charge carriers. The lowest resistivity value- $1.33x10^{5}$ Ω-cm was observed for the film annealed at 250°C with nitrogen atmosphere, and the resistivity increases as a function of annealing temperature. For the samples annealed in a nitrogen-sulfur atmosphere, the resistivity value decreases as the annealing temperature increases, and the obtained lowest resistivity value was $1.74x10^{5}$ Ω-cm (350°C). In both atmospheres, the mobility increases as a function of the temperature, and the values are similar for both cases, except for the film annealed at 350°C in a nitrogen atmosphere where the highest value of 65 cm^2 $V^{-1}s^{-1}$ was achieved.

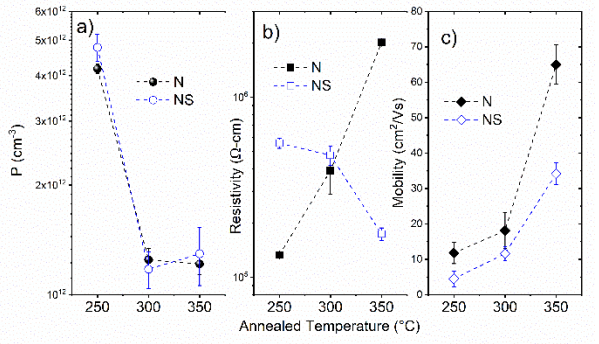

Fig. 4. Hall effect measurement of the samples annealed in nitrogen and nitrogen-sulfur atmospheres vs temperature a) hole concentration, b) resistivity and c) mobility.

IV. CONCLUSIONS

The Sb_2S_3 thin films were successfully annealed under nitrogen and nitrogen-sulfur atmospheres. The samples annealed at 250°C in both nitrogen and nitrogen-sulfur atmospheres were polycrystalline in nature, which was confirmed by XRD and Raman. The films annealed with nitrogen-sulfur atmosphere exhibited better properties. The transmission was increased up to 10 %. The band gap of the samples was tuned from 1.74 to1.82 eV as a function of annealing temperature. All the films showed p-type conductivity and the maximum charge carrier concentration of $4.8x10^{12}$ cm^{-3} was observed for the film annealed at 250 °C under nitrogen-sulfur atmosphere. To better our knowledge, the annealing treatment in an N-S atmosphere work is not yet published for Sb_2S_3 thin films.

ACKNOWLEDGEMENTS

The authors acknowledge the Fondo Química Somos Todos 2021-FQ-UAQ for the financial support.

V. REFERENCES

[1] J. Escorcia-García, D. Becerra, M.T.S. Nair, P.K. Nair, Heterojunction CdS/Sb_2S_3 solar cells using antimony sulfide thin films prepared by thermal evaporation., Thin Solid Films., 569 (2014) 28–34.

[2] R.G. Sotelo Marquina, T.G. Sanchez, N.R. Mathews, X. Mathew., Vacuum coated Sb_2S_3 thin films: Thermal treatment and the evolution of its physical properties., Mat. Res. Bull., 90 (2017) 285-294.

[3] C. Gao, J. Huang, H. Li, K. Sun, Y. Lai, M. Ji, L. Jiang, F. Liu., Fabrication of Sb_2S_3 thin films by sputtering and post-annealing for solar cells., Cer. Inter., 45 (2019) 3044-3051.

[4] U. Chalapathi, B. Poornaprakash, Chang-Hoi Ahn, Si-Hyun Park., Large-grained Sb_2S_3 thin films with Sn-doping by chemical bath deposition for planar heterojunction solar cells., Mat. Sci. Sem. Proc., 84 (2018) 138-143.

[5] M.S. You, C.S. Lim, D.H. Kwon, J.H. Heo, S.H. Im, K.J. Chae., Oxide-free Sb_2S_3 sensitized solar cells fabricated by spin and heat-treatment of Sb(III) (thioacetamide)$_2Cl_3$., Org. Electron. Phys. Mater. Appl., 21 (2015) 155–159.

[6] M.Y. Versavel, J.A. Haber., Structural and optical properties of amorphous and crystalline antimony sulfide thin-films., Thin Solid Films., 515 (2007) 7171–7176.

[7] M. I. Medina-Montes, E. Campos-González, M. Morales-Luna, T. G. Sánchez, M. Becerril-Silva, S. A. Mayén-Hernández, F. de Moure-Flores, J. Santos-Cruz., Development of phase-pure $CuSbS_2$ thin films by annealing thermally evaporated CuS/Sb_2S_3 stacking layer for solar cell applications", Mater. Sci. in Semicond. Process., 80 (2018) 74-84

[8] J.S. Eensalu, A. Katerski, E. Kärber, A.I. Oja, A. Mere, M. Krunks., Uniform Sb_2S_3 optical coatings by

chemical spray method., Beilstein J. Nanotechnol., 10(2019) 198-210.

[9] Y. Liu, K.T. Eddie Chua, T.C. Sum, C.K. Gan., First-principles study of the lattice dynamics of Sb_2S_3., Phys. Chem. Chem. Phys., 16 (2014) 345–350.

[10] J. Ibáñez, J.A. Sans, C. Popescu, J. López-Vidrier, J.J. Elvira-Betanzos, V.P. Cuenca-Gotor, O. Gomis, F.J. Manjón, P. Rodríguez-Hernández, A. Muñoz., Structural, Vibrational, and Electronic Study of Sb2S3 at High Pressure., J. Phys. Chem. C., 120(**2016)** 10547–10558.

[11] D. Santos-Cruz, S.A. Mayén-Hernández, F. de Moure-Flores, J. Campos-Álvarez, M. Pal, J. Santos-Cruz., CuO_x thin films by direct oxidation of Cu films deposited by physical vapor deposition., Res. In Phys., 7 (2017) 4140-4144.